Heliyon 9 (2023) e17923

Contents lists available at ScienceDirect

Heliyon

journal homepage: www.cell.com/heliyon

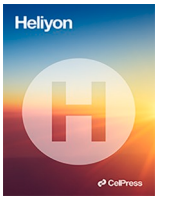

Effect of case hardening on the wear and hardness properties of medium carbon steel for bone crushing application

Bose M. Edun [a,b,*], Oluseyi O. Ajayi [b], Philip O. Babalola [b], Enesi Y. Salawu [b]

[a] Department of Mechanical Engineering, Ogun State Institute of Technology, Igbesa, Nigeria
[b] Department of Mechanical Engineering, Covenant University, Ota, Nigeria

ARTICLE INFO

Keywords:
Wear resistance
Fatigue strength
Carburisation
Case hardening
Microstructure
Transformation
Strengthening
Crushing application
Economic proficiency

ABSTRACT

The majority of wear-related problems are connected to crushing machines because hammer failure frequently causes machine failure which eventually leads to machine downtime. Therefore, improving the reliability of crushing materials is necessary for effective production. This research investigation focused on the development of crushing material with appropriate strength properties that can function in critical, impact-prone, corrosive, and abrasive conditions. The current study used palm kernel shell, coconut shell, and sawdust powder as the media for medium carbon steel in order to valorize the agro waste. Carburising media PKS-composition, *CS*-composition, and SD-composition were changed to 40%: 30%: 30%, PKS-composition 100%, *CS*-composition 100%, and SD-composition 100%. The process was carried out in 1 h (60 mims), 1 h:30 min (90 min), 2 h (120 min), 2 h:30 (150 min), and 3 h (180 min) soak period with varied carburising temperatures of 900, 950, 1000, and 1050 °C. However, several characterisation and mechanical tests were carried out using an optical microscope, a spark spectrometer, a scanning electron microscope coupled with an energy dispersive spectrometer, wear tester to explore their microstructural features. Vicker's hardness tester, sliding wear tester, and a thermal gravimetric analysis testing machine were also employed. In order to establish reasons for failure other than the cyclic loading on the materials, the results were compared with the properties of as-received un-failed, and carburised medium carbon steel. The results of carburisation show that PKS penetrates carbon at a rate that is noticeably higher than that of other materials at various temperatures and times, indicating that carbon diffuses deeply into the material. Hence, this enhances the wear resistance, and sample's hardness number but decreased its impact toughness respectively.

1. Introduction

The exigency for carbon steel components is rapidly rising in terms of flexibility, weldability, and cost-effectiveness in manufacturing industries [1]. In many different types of wear environments, high-strength abrasion-resistant steels are frequently employed. It can reduce wear-related failure lowering the rate at which mechanical parts abrade, hence improving service life [2]. One of the most important surface features of medium carbon steel parts is their wear resistance. Brittle fracture brought on by abrasive

* Corresponding author. Department of Mechanical Engineering, Covenant University, Ota, Nigeria.
E-mail addresses: bosemosunmola@yahoo.com (B.M. Edun), oluseyi.ajayi@covenantuniversity.edu.ng (O.O. Ajayi), philip.babalola@covenantuniversity.edu.ng (P.O. Babalola), enesi.salawu@covenantuniversity.edu.ng (E.Y. Salawu).

https://doi.org/10.1016/j.heliyon.2023.e17923
Received 6 March 2023; Received in revised form 28 June 2023; Accepted 1 July 2023
Available online 7 July 2023

Nomenclature

MCS	The Medium carbon steel
PKS	Palm kernel shell-composition
CS	Coconut shell-composition
SD	Saw dust-composition
Hr	Hours
Mins	Minutes
wt%	Weight percentage
μm	Micron
ASTM	American Society for Testing and Materials
HCL	Hydrogen chloride
SES	Spark emission spectrometer
SEM	The Scanning electron microscope
EDS	The Energy Dispersive Spectrometer
TEM	The Transmission Electron Microscope
3D	3 Dimension surface plot

wear damaged wear mechanisms in MCS. However, metallic materials' surface hardness and wear resistance are increased through techniques that expose the surface to carbon. This is done to achieve a certain desired set of properties to maximize their life and function at their best in their intended service applications. Hence, steel parts' wear resistance is increased via surface hardening [3] Recent research has shown that as these parts constantly experience dynamic loads, they should be resistant to impact and abrasive wear. Hence, martensitic steels with low content of potentially harmful elements (P and S) exhibit both high strength indices and acceptable plastic characteristics to withstand continuous stress which may possibly cause failure [4,5] Researchers have also found metal matrix composites, and these materials use silicon nitride, boron nitride, alumina, and titanium carbide as reinforcement materials. Thus, the use of reinforcing materials aims to improve the overall attributes of the selected material, including its mechanical, thermal, compression, and tensile strength, yield strength, toughness, good processing capabilities, and economic proficiency (efficiency) [6]. However, due to the obtainability and incredibly low cost of obtaining the proposed agro waste, the usage of organically sourced particles (organic waste) has been shown to be a valuable resource and a very good strengthening ingredient [7]. The carburisation method is more promising than conventional heat treatment processes. Typically, during the carburisation process, carbon atoms diffused into the low-carbon steel's crystal lattice, generating lattice strain and increasing the strength properties of the metal. It causes the carbon steels to be hardened, and exhibit greater strength and toughness, which typically leads to the transformation of surface and low core strength of the metal steels. The technique also leads to the development of a novel microstructure consisting of a homogeneous dispersion of carbon particles in an ultrafine-grained martensitic matrix [8–10] examined how the distribution of carbon altered the tribological behavior of the carburised mild steel with varied carburising times. The increase in carburising time from 1hr:3hr brought about an increase martensite content and the hardness of the sample. Hence, an improved anti-wear oxide is produced due to a transformation in the properties of the material. Longer carburising time also produced wider martensite and narrow grain boundaries with fewer precipitates, increasing the steel's resistance to fracture.

Case hardening is a conventional method used to create steel components with a hard surface and ductile core. The surface's carbon gradient causes the variation in transformation behavior while the martensite transformation into ferrite, pearlite, and bainite is also influenced by the process. If quenching is done immediately following, austenite will change into martensite and remain as retained austenite at room temperature [11]. Austenitizing, or obtaining homogeneous austenite at the proper temperature within the austenite stability range, is usually the initial stage in steel heat treatment methods. Steels must be heated to the austenitizing temperature range for a long enough amount of time to completely transform into austenite and achieve homogeneity in composition. This is referred to as carbon leveling in the industrial world. The product suffers because of insufficient carbon leveling, which causes places with more carbon to change into martensite while those with less carbon change into bainite [12]. [13], reported, that the surface and structural characteristics of carbon steels are altered when subjected to various heat treatments. They noted that the impact toughness of the case-hardened steel samples reduced while the quantity of carbide in the steels increased with increased carbon content. The addition of carbon derived from organic wastes into the as-received sample produces a sample with an outstanding combination of strength properties for long service compared to the as-received sample. Thus, this study explores the impact of pulverized organic carbon (palm kernel shell, coconut shell, and sawdust powder) on the mechanical characteristics of medium carbon steel material for crushing applications. This helps in determining the effect of case hardening on the efficiency of the crushing material. Also, encourages agro-waste valorization, which will lessen environmental contamination. SDG 11 (Sustainable Cities and Communities) being a crucial part of Sustainable development.

2. Methodology

2.1. Materials

The material under investigation is a failed crushing material obtained from feedmill factory at Abeokuta Ogun State, Nigeria. The conventional material is MCS purchased from an open market Owode, Onirin. The crushing material failed as a result of the repeated blows it often experienced which eventually led to abrasive, fatigue, and erosive wear.

2.2. Procedural steps of the experiment

In the preparation of mechanical specimens (samples) using abrasive particles, the material is removed from the surface in progressively finer steps until the desired result is obtained. This is required to ensure that the surface is free of impurities and cracks for proper observation of the samples. A hacksaw was carefully used to section the as-received hammer to dimensions (40 mm × 30 mm × 10 mm) to avoid structural distortion. After the preparation process, media were finely crushed using the pulverisation method, sieved with 75 μm added then placed in the muffle furnace of 1500 °C capacity. The hammer materials under investigation (as-received steels) were taken from a feed mill and cleaned with silicon carbide P1200 abrasives in accordance with ASTM standards while 4% HCL was used for etching purposes in order to reveal the cracks on the surface. This provides a polished and smooth surface for simple carbon diffusion into the steel's surface. On each as-received and carburised sample, a Spark emission spectrometer (SES) (Bruker) with the model number Q4 TASMAN was utilized to conduct a chemical composition analysis. The spectrometer was put to use while a plasma was created when a high-energy spark between the material and the electrode was released into an argon atmosphere. Further to the elemental composition analysis, the microstructures were examined using an optical microscope to study the morphology of the samples. Similarly, a Scanning electron microscope (SEM) coupled with an Energy Dispersive Spectrometer was employed to present the microstructure and examine the micro surface structure of metal samples. The use of a Transmission Electron Microscope (TEM) allowed the most in-depth structural data or information to be obtained at the highest resolution possible, which SEM is unable to provide. Tables 1–3(a–c) provides the list of the researched steel's composition analysis. Vicker's Hardness Tester, sliding wear tester, and thermal gravimetric analysis testing machine were also employed. ImageJ software was used to analyse the 3D surface plot of the SEM and TEM results. Samples were heat treated at different temperatures, and time followed by water quenching, in order to maximize the impact of the heat treatments on the microstructure, and the useful life of the examined steels. The heating rates were set at 1 h (60 min), 1 h:30 min, 2 h (120 min), 2 h:30 min, and 3 h (180 min) with various temperatures of 900, 50, 1100 (°C) respectively. Hence, the carbon diffusion rate is high during the heat treatment process with carbon being retained. The study produced a medium carbon steel hammer material for bone crushing that has been bio-carbon functionalised for better mechanical and tribological properties. It showed that the diffusion of carbon from the palm kernel shell penetrates deeper into the core metal surface and affects greater strength and tribological qualities.

3. Result and discussion

3.1. Elemental chemical analysis of the as-received medium carbon steel (failed, un-failed and carburised)

The chemical composition tests of the as-received medium carbon steel (un-failed and failed) are presented in Table 1 (a–c) and Table 2 (a–c) with 0.547% and 0.467% carbon contents. Manganese has a greater impact on hardenability than other alloying elements. It is also likely to speed up the carbon penetration rate during the procedure. Comparatively, the elemental compositions of carbon present in the mild steel and mediun carbon steel (failed) were less than that of the un-failed medium carbon steel that is being used as a control. Therefore, the choice of medium carbon steel was made for this study for functionalization. In steel metals, silicon is a graphite stabilising constituent, which means it helps the alloy develop graphite rather than iron carbide. As a result, the silicon content indicates the necessity for steady graphite flake production. Table 3(a-c) also displays the chemical compositions of carburised medium carbon steels based on different organic carburisers according to Voige's law mixtures. The mixture of 40 (wt%) pulverised palm kernel shell, 20 (wt%) pulverised coconut shell, 20 (wt%) pulverized sawdust, and 20 (wt%) pulverised eggshell at 900 °C, 950 °C, and 1000 °C for the same carburisation was employed. Therefore, based on the composition analysis of the sample's chemical components, it can be concluded that these compositions were similar to the outcomes of separate carburisation experiments utilizing

Table 1
Depicts the chemical composition of the as-received failed medium carbon steel.

Element	Carbon	Silicon	Manganese	Phosphorus	Sulphur	Chromium
Composition %	0.467	1.98	0.753	0.0214	0.0249	0.0891
Element	Molybdenum	Nickel	Aluminium	Cobalt	Copper	Niobium
Composition %	0.0118	0.136	0.0339	0.00146	0.242	0.00100
Element			Iron (Fe)			CEQ
Composition %			96.1			0.635

Table 2
Chemical composition of the as-received medium carbon steel (un-failed).

Element	Carbon	Silicon	Manganese	Phosphorus	Sulphur	Chromium
Composition %	0.547	1.84	0.876	0.0194	0.0193	0.0116
Element	Molybdenum	Nickel	Aluminium	Cobalt	Copper	Niobium
Composition %	0.00100	0.136	0.0116	0.0049	0.043	0.00100
Element			Iron (Fe)			CEQ
Composition %			96.5			0.718

Table 3
Chemical composition of the sample subjected to carburisation using palm kernel shell at 1050 °*C* for 180 min.

Element	Carbon	Silicon	Manganese	Phosphorus	Sulphur	Chromium
Composition %	1.470	1.983	0.875	0.0213	0.0246	0.0889
Element	Molybdenum	Nickel	Aluminium	Cobalt	Copper	Niobium
Composition %	0.00100	0.135	0.0115	0.0048	0.048	0.00100
Element			Iron (Fe)			CEQ
Composition %			90			0.718

each carburiser at different temperatures and times (1050 °C and 1100 °C for 3 h). Due to the higher nickel concentration and higher chromium content, the sample is more ductile, malleable, and formable, and its corrosion resistance is enhanced. The declining volume ratio of each carburiser, however, slows the rate of carbon diffusion [14]. [15], reported that the presence of silicon, manganese, and chromium enhances the wear resistance of the surface but, the percentage of manganese present is less compared to that of as-received medium carbon steel hammer material. Also, the hardness of the steel increased, and the sliding wear rate reduced with increasing amounts of C from 0.30 to 0.36 wt%, Mo from 0.5 to 0.8 wt%, and Ni from 0 to 2.5 wt% [16]. The higher percentage of sulphur and phosphorus concentrations, in Fig. 1 as compared to each other, lowers toughness, which could lead to the occurrence of brittle fracture that is, the failure of the hammer. More so, hardness declines monotonously with increasing sulphur content due to the action of sulfides on void nucleation [17]. Hence, the material's susceptibility to wear increases. Comparatively, it was observed that the proportion of iron decreased while the percentages of carbon, chromium, nickel, and manganese increased as shown in Table 3(a-c). This demonstrates that the material has more strength and hardness. Manganese hence affects hardenability more than other alloying components. Additionally, it might hasten the rate at which carbon penetrates during the process. Hence, medium carbon steel was selected for this study. As a graphite stabilising component in steel alloys, silicon aids in the alloy's development of graphite rather than iron carbide. Silicon functions as a "graphite stabilising element" in steel alloys, encouraging the alloy's development of graphite rather than iron carbide. As a result, the silicon content suggests the need for the consistent manufacture of graphite flakes. The chemical compositions of medium carbon steels that have been carburised employing various organic carburisers are shown in Table 3 (a-c). Comparatively, it was noted that there was a reduction in the percentage of iron while the percentage of carbon, chromium, nickel, and manganese are more as presented in Table 3(a-c). This shows that the strength and hardness of the material are improved.

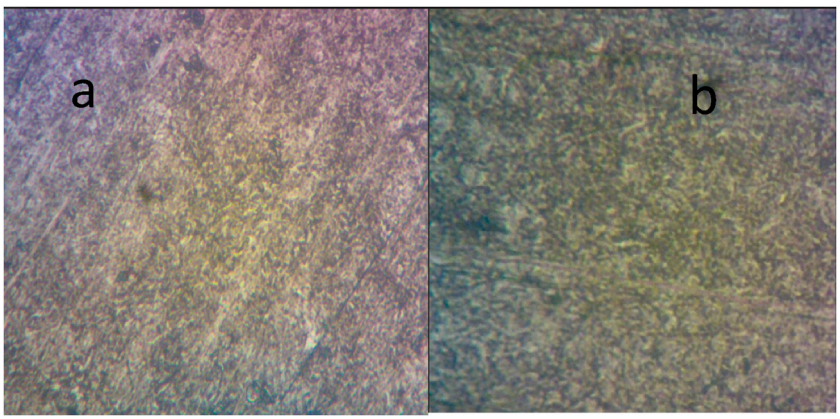

Fig. 1. Optical microstructural feature of as-received medium carbon steel (a) (un-failed) (b) carburised.

3.2. Microstructural analysis medium carbon steel (un-failed and carburised)

The optical micrographs of the as-received investigated medium carbon (un-failed and carburised) steels are displayed in Fig. 1(a and b). Both of the studied steels, as shown in this figure, contain an austenitic matrix and secondary carbides (C1) precipitated at the grain boundaries. Manganese is a weak carbide-forming element; it dissolves only in cementite and lowers the carbon activity in austenite without producing any carbides of its own. Carbon cannot be completely maintained in a solid solution when present in significant quantities. Therefore, low-concentration chromium addition encourages iron and manganese to replace the latter to create alloyed cementite (Fe,Mn,Cr).

3.3. Scanning electron microstructure coupled with Energy Dispersive Spectroscopy analysis of the samples

Figs. 2 and 3 display the SEM microstructure and EDX of the as-received failed medium carbon steel sample. Similarly, Figs. 4 and 5 showed the SEM microstructure and EDX of the as-received failed mild steel sample. Figs. 6 and 7 also showed the SEM microstructure and EDX of the as-received medium carbon steel (control) sample before carburisation. The TEM Micrograph and 3D surface plot image of the steel sample carburised with palm kernel shell at 1050 $^{\circ}C$ for 3 h (180 min) are displayed in Fig. 8(a and b). It was noted that graphite predominates on the metal surface in Figs. 9–12, which is related to the type of carbon content utilised in the carburisation process. The microstructure of the sample at 1050 °C for 3 h (180 min) is further illustrated in Fig. 11. As shown in Figs. 9, 11 and 13 for samples that were for 1 h and 1 h:30 min, respectively, the surface was seen to have an enhanced precipitate of carbon. On the other hand, graphite precipitates began to appear on the metal surface around 180 min (Fig. 12). Due to the presence of graphite, it can be concluded that during the carburisation process, diffusion actually occurred at a higher and faster rate at 1050 °C for 3 h (180 min).

3.4. SEM/EDS analyses of as-received failed medium carbon steel

The SEM/EDS microstructure of the as-received failed medium carbon steel at a distinctive numerical aperture of the microscope optical system is presented in Figs. 2 and 3. The surface was observed being dominated by pearlite, having oxide layers in the form of corrosion deposits. The heat-treated samples are made up of martensite, residual austenite, and a tiny amount of precipitates. The investigated steel is more easily hardenable and is more conducive to the martensitic transformation as the heat treatment temperature is raised and alloying elements (C, Cr, Ni, Nb) present in the media are added. The EDS in Fig. 3 showed that iron, magnesium, zinc and chlorine were major elements present. The low percentage of nickel, silicon, and absence of chromium, and manganese contributed to the failure of the sample.

3.5. SEM/EDS analyses of as-received failed mild steel

Fig. 4 revealed the surface morphology of as-received failed mild steel when the visuals or images were scaled up. Corrosion deposits in form of dark spot locations and oxides were observed on the surface of the sample because of the porosity of the structure and presence of oxygen and water. Also, Fig. 5 depicts the EDS result which indicated that iron, nickel, sulphur, zinc, chlorine, chromium, silicon, and phosphorus were present with iron having the highest wt %.

3.6. SEM/EDS analyses of as-received medium carbon steel (control) before the carburisation process

Fig. 6 shows the medium carbon steel (control) sample in its uncarburised state. According to the EDS results displayed in Fig. 5, the sample mostly composed of iron and oxygen, with smaller amounts of silicon, aluminum, chromium, zinc, chlorine, sulphur, and copper. This outcome aids in comprehending how the mild steel and medium interact. The medium carbon steel material's initial state prior to the carburisation process could be seen in the morphology in Fig. 6.

3.7. SEM/EDS analyses of as received medium carbon steel carburised with palm kernel shell at 900 °C for 1 h (60 min)

The SEM/EDS morphology and 3D surface plot image of a medium carbon steel sample carburised with finely ground palm kernel

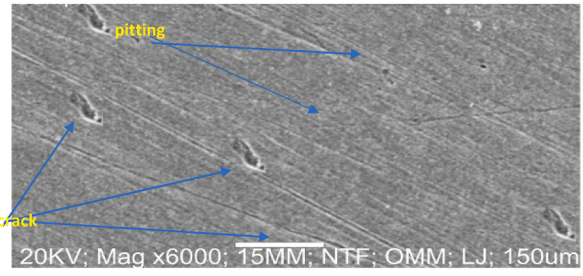

Fig. 2. Micrograph showing the surface morphology of as-received failed medium carbon steel sample.

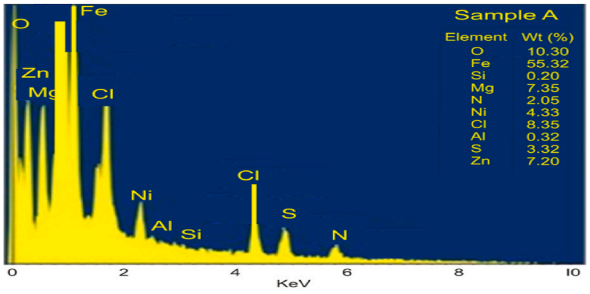

Fig. 3. Energy Dispersive Spectroscopy of the elements in failed medium carbon steel sample.

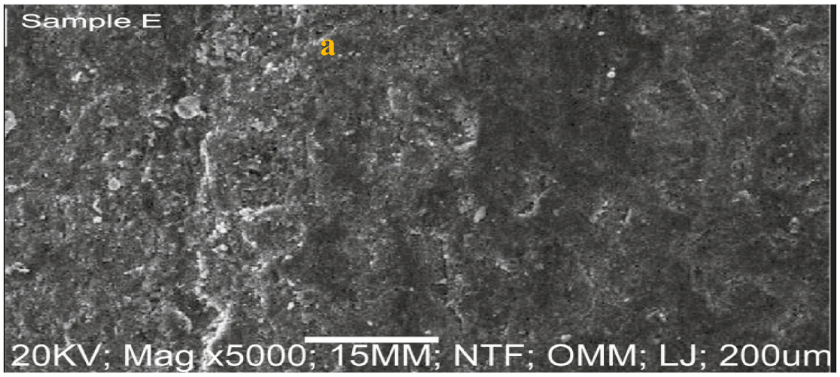

Fig. 4. Micrograph showing the surface morphology of the as-received failed mild steel sample.

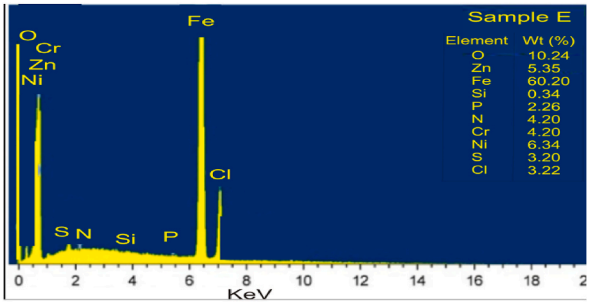

Fig. 5. Energy Dispersive Spectroscopy of the elements of the as-received failed mild steel sample.

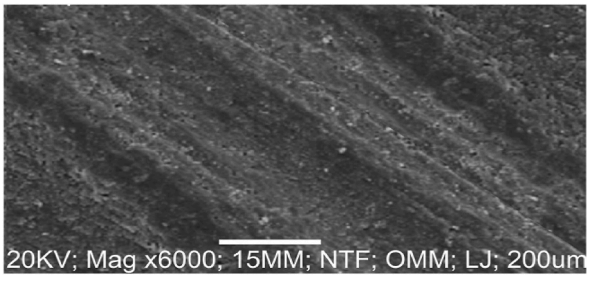

Fig. 6. Micrograph showing the surface morphology of the as-received medium carbon steel sample (control).

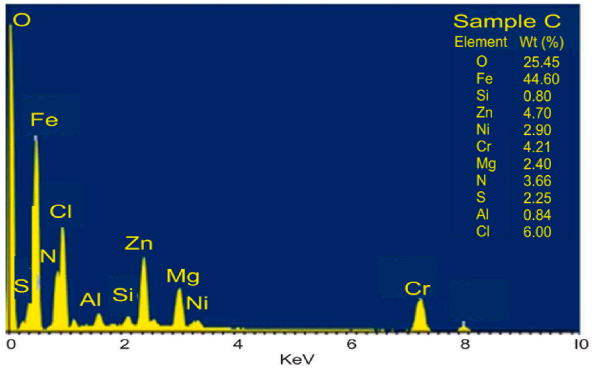

Fig. 7. Energy Dispersive Spectroscopy of the elements of the as-received medium carbon steel sample (control).

shell at a temperature of 900 °C is shown in Fig. 8(a-c). There was graphite formation on the material's surface which aids in the carbon retention. The EDS result showed that different elements were present in variable amounts. The carbon spread into the sample, indicating the mechanisms through which graphite is formed.

3.8. SEM/EDS analyses of as received medium carbon steel carburised with palm kernel shell at 950 °C for 1 h (60 min)

Fig. 9(a–c) depicts the SEM/EDS morphology and 3D surface plot image of a medium carbon steel sample that was carburised at 950 °C with finely ground palm kernel shell. More graphite layers were found to dominate the sample's surface, which aids in the explanation of the mechanism by which graphite is formed at temperatures and times. In the same vein, the carbon diffusion rate in the 3D image of the transmission electron microstructural feature of the steel sample is low when compared with the 3D image of sample carburised with palm kernel shell at 1050 °*C* for 3 h

3.9. SEM/EDS analyses of as received medium carbon steel carburised with coconut shell, palm kernel shell, and sawdust at 900 °C for 1 h (60 min)

Furthermore, Fig. 10(a-c)shows the SEM/EDS morphology and 3D image of the transmission electron microstructural feature of the sample that was carburised at a temperature of 900 °C for 1 h while being mixed with sawdust, palm kernel shell, and crushed coconut shell. When the mixing ratio of 40 (wt. %) of pulverised palm kernel shell, 20 ((wt. %)) of pulverised coconut shell, 20 ((wt. %)) of pulverised sawdust, and 20 ((wt. %)) of pulverised eggshell was used, the mechanism of graphite formation was different from that seen in Figs. 8 and 9. Due to numerous elements seen in the morphology, there is evidence that the sample was improved during the carburisation process.

3.10. SEM/EDS analyses of as received medium carbon steel carburised with coconut shell, palm kernel shell, and sawdust at 950 °C for 1 h:30 min

Fig. 11(a–c) shows the SEM/EDS morphology and 3D image of the transmission electron microstructural feature of the sample after it was heated to 950 °C for 1 h:30 min and with sawdust, palm kernel shell, and crushed coconut shell. The same mixing ratio shown in Fig. 10 above also results in a material's surface being dominated by graphite. Additionally, a number of elements were seen in the EDS result, indicating that elements from the fluid had diffused into the sample material.

3.11. SEM/EDS analyses of as-received medium carbon steel carburised with palm kernel shell at 1050 °C for 3 h (180 min)

The SEM/EDS morphology of a medium carbon steel sample with a finely crushed palm kernel shell at 1050 °C for 3 h is shown in Fig. 12(a–c). Similarly, the graphite that developed on the material's surface helped to maintain and aid carbon diffusion. The ferrite phase, which is iron-rich, and the darker portions, which indicate the presence of carbon in the pearlite phase, which was composed of alternate stripes of ferrite and cementite, were generally used to show the changes (carbon-rich). The percentages of various components in EDS results vary. This may be connected to certain components in the media. Silicon, carbon, potassium, calcium, iron, aluminum, and oxygen make up the majority of the elements that make up PKS. Copper, phosphorus, and silicon may also be present in PKS. There may be traces of rubidium, nickel, manganese, chromium, and titanium among the elemental elements. As the rate of penetration is significantly higher when compared to other materials at various temperatures and times, the depth of carbon diffusion into the material is evident. Additionally, during the carburisation process, a thin, soft layer was created on the surface as a result of the oxidation of alloying metals like Cr and Mn. In the same vein, the internal oxidation prevented the presence of a higher value of sulphur content and increases the machinability of the material, while nickel improves hardenability, toughness, ductility, and corrosion resistance. Nickel also acts as an antitrust. Similarly, the presence of tin increases the material's resistance to corrosion and improves

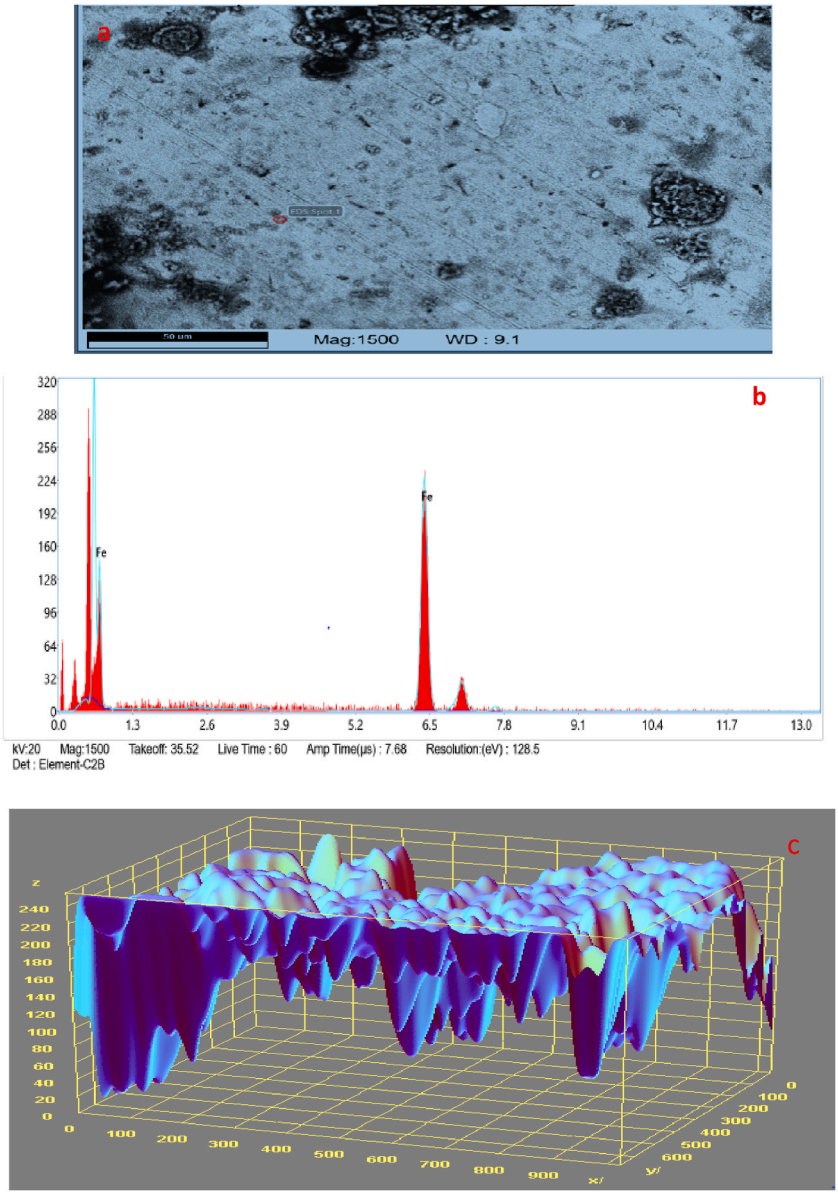

Fig. 8. a. Micrograph of medium carbon steel carburised with palm kernel shell at 900 °*C* for 1 h. b. Energy Dispersive Spectroscopy of the elements c. 3D surface plot image of the scanning electron microstructural feature of the steel sample carburised.

hardness and strength. Also, titanium and tungsten increase corrosion resistance while tungsten further increases the wear resistance and melting temperature. Because of the oxidation process, hardenability, and high-temperature strength, the presence of chromium (Cr) improves corrosion resistance. It benefits from the application as a crushing component because of its capacity to boost high-temperature strength. Additionally, weldability and machinability are enhanced by the presence of an insignificant percentage of sulphur. The addition of calcium (Ca) to low-carbon steel can increase its resistance to hot cracking and weld-related cracking, while the inclusion of Magnesium (Mg) increases toughness and resistance to cracking (which can be caused by the effects of other elements present).

The elemental composition percentage is displayed in the EDS profile in Fig. 12(b). The main elements dispersed into the material as observed were Fe, Si, C, Mn, Zn, S, and Cl. The hardness and strength of the material hence increased due to the manganese Mn present in the structure which shows the formation of pearlite at the interface as a result of the cooling of austenite that is gamma-phase iron (γ-Fe). In general, the hardness of the carburised steel rises as carbon content does too, but fracture toughness falls as carbon content rises. On the other hand, the percentage of chromium Cr present boosts the samples' wear resistance, hardenability, resistance to oxidation, and resistance to corrosion [18]. Additionally, it is believed to be the effect of variations in Si levels between these two materials. Iron tends to get stronger when Si dissolves in it. Axles, crankshafts, couplings, and gears are some of the heavy machinery

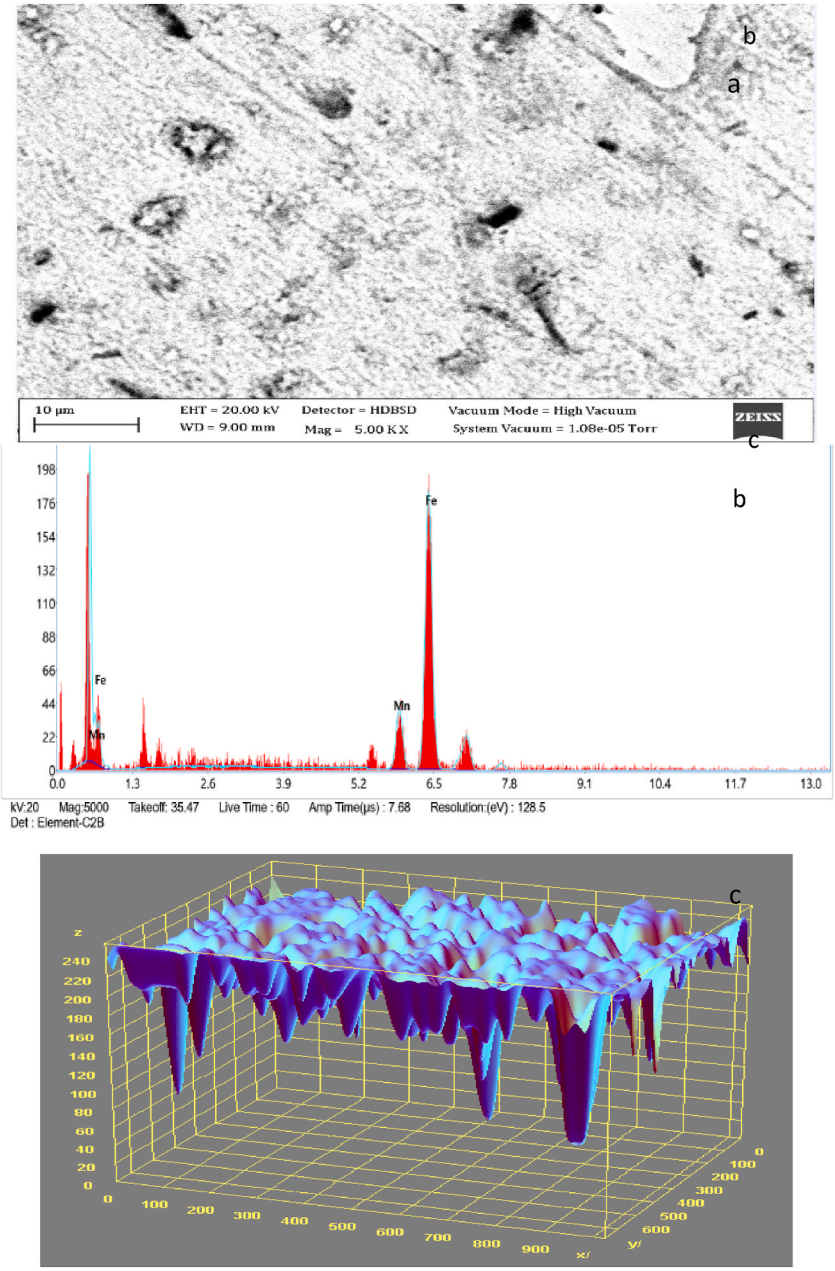

Fig. 9. a. Micrograph of medium carbon steel carburised with coconut shell at 950 °*C* for 1 h:30 min. b. Energy Dispersive Spectroscopy of the elements. c. 3D surface plot image of the scanning electron microstructural feature of the steel sample.

components that frequently make use of medium carbon steel. Following the carburisation process, the microstructure becomes hard, increasing the material's hardness and tensile strength while decreasing its ductility. However, the amount and rate of diffusion of carbon in the steel sample were higher which affects the martensite's hardness as shown in Fig. 12(c). This is due to the fact that hardness increases with carbon content at an elevated temperature and time [19]. Intercritical heat treatment, also known as high-temperature heat treatment, is a quick and easy approach to creating ferrite/martensite dual-phase microstructure, which balances steel's ductility and strength. The final qualities of the sample during the carburisation process were improved at 1050 °*C* for 3 h temperature and duration

3.12. SEM/EDS analyses of as received medium carbon steel carburised with palm kernel shell at 1000 °C for 3 h (180 min)

Fig. 13(a–c) presents the SEM/EDS results of the sample that was carburised with pulverized palm kernel shell at a temperature of

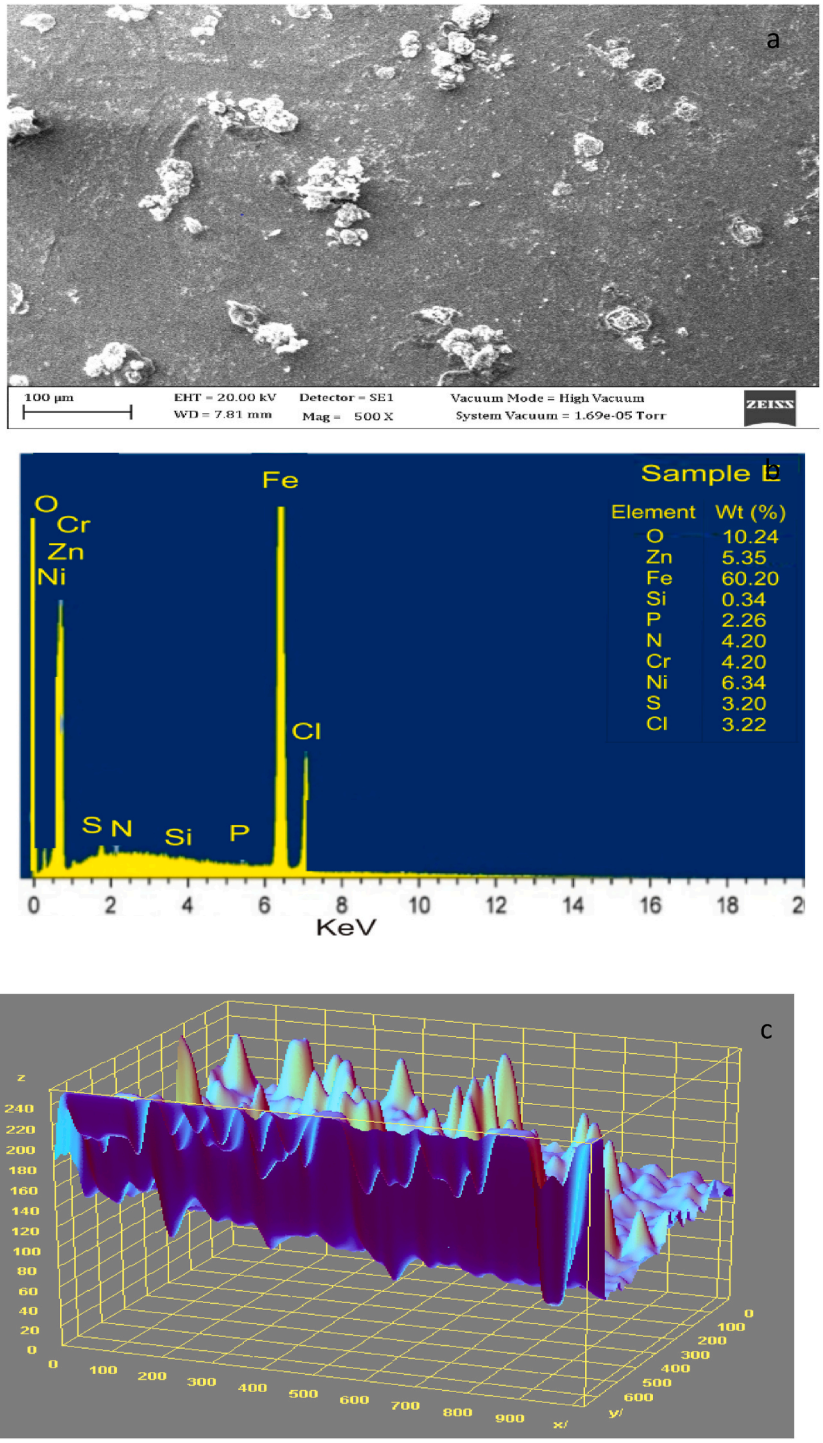

Fig. 10. a. Micrograph of medium carbon steel carburised with sawdust, coconut shell, and palm kernel shell at 900 °*C* for 1 h b. Energy Dispersive Spectroscopy of the elements c. 3D surface plot image of the scanning electron microstructural feature of the steel sample carburised.

1000 °C. Similar to Figs. 11 and 12, the surface was dominated by graphite. Similarly, the graphite that developed on the material's surface helped to maintain and aid carbon diffusion. The percentages of various components in EDS results vary. This was done so that the strength qualities could be compared to those of tests done at various temperatures and times, as well as to those of samples carburised using different media. The EDS results showed a number of components that point to the presence of diffusion during carburisation.

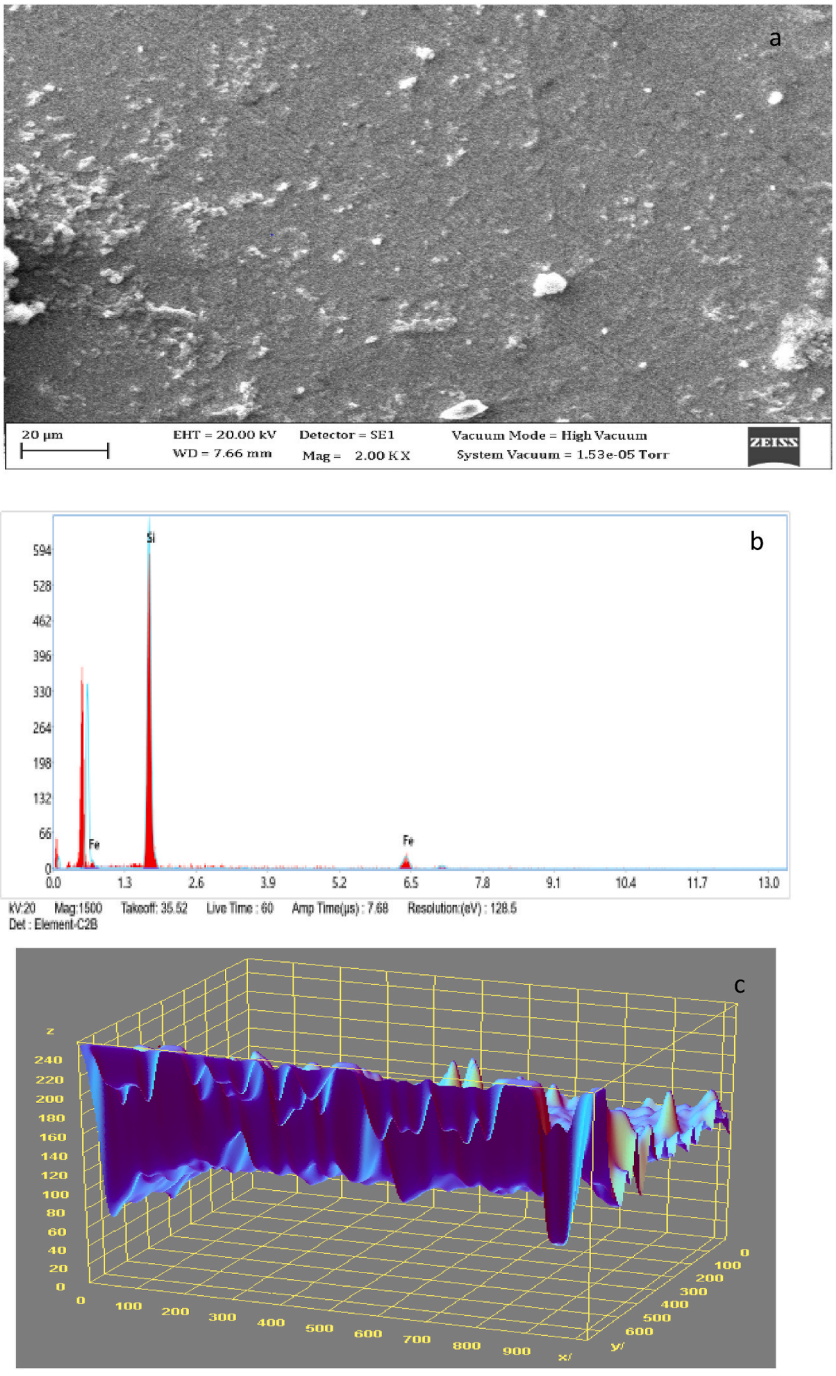

Fig. 11. a. Micrograph of medium carbon steel carburised with sawdust, coconut shell, and palm kernel shell at 900 °*C* for 1 h:30 min. b. Energy Dispersive Spectroscopy of the elements c. 3D surface plot image of the scanning electron microstructural feature of the steel sample carburised.

3.13. TEM analyses of as received medium carbon steel carburised with palm kernel shell at 1050 °C for 3 h (180 min)

Fig. 14(a and b) represents the transmission electron microscope results and 3D image of the carburised steel samples employed in the study. It shows the topography, morphology as well as crystalline details of the carburised sample at the best possible resolution. It was revealed that the heat-treated surface is composed of a continuous oxide layer, followed by a complicated interior oxidation layer which is formed with the homogenous carbon content, where Cr and Mn oxides were discovered to occupy grain boundaries in a globular form in the locale of the surface. A network of grain boundaries is generated from Si oxides at greater depths as the transformation moves inwardly and outwardly. Thus at the initial stage, the process for 3 h, 1050 °C with finely crushed palm kernel shell),

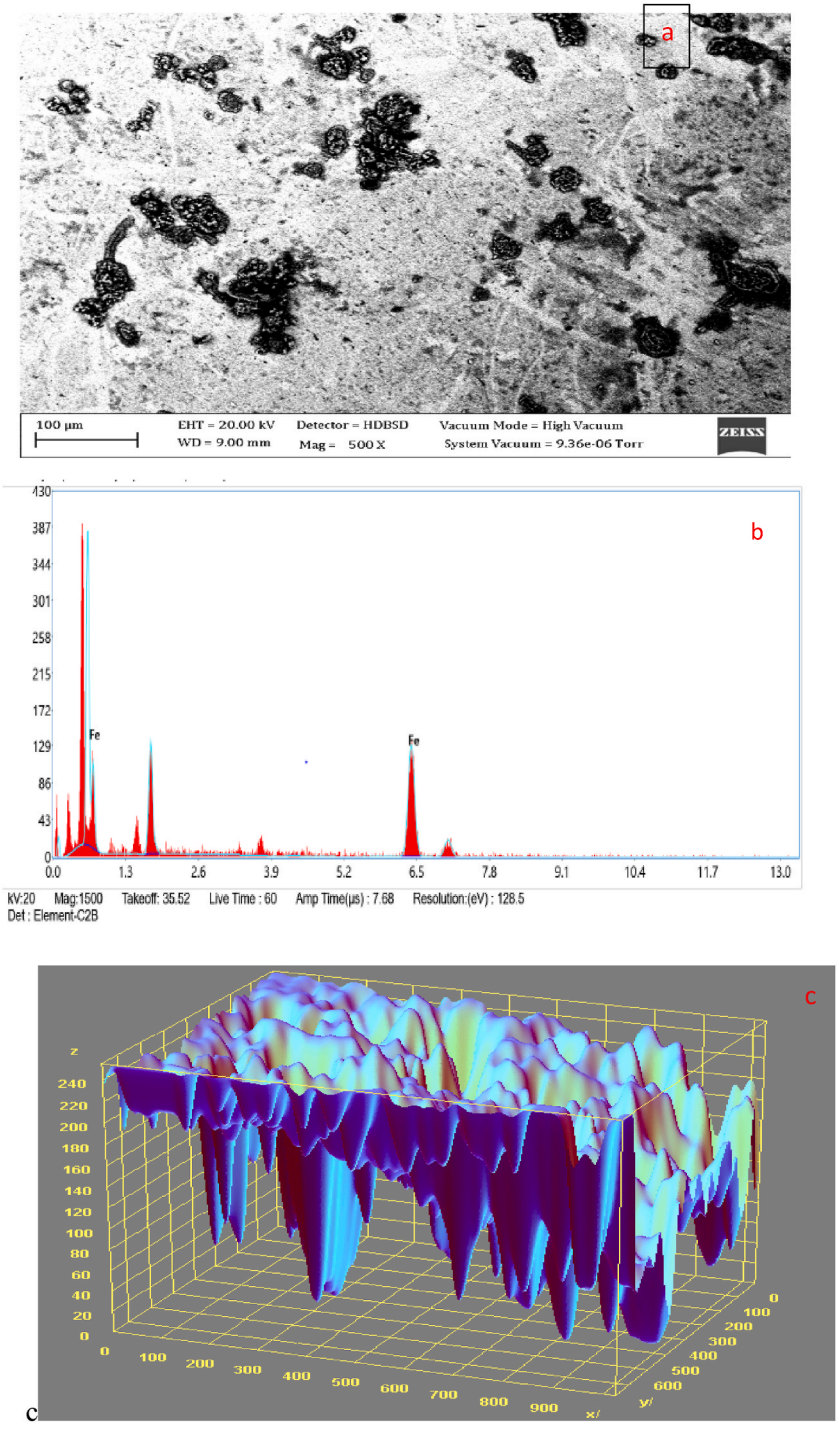

Fig. 12. a. Micrograph of medium carbon steel carburised with palm kernel shell at 1050 °*C* for 3 h. b. Energy Dispersive Spectroscopy of the elements c. 3D surface plot image of the scanning electron microstructural feature of the steel sample.

increased at a faster rate with the formation of internal oxides (mostly complex oxides) as compared with the samples at reduced time and temperatures.

3.14. Hardness

Figs. 15 and 16 display the hardness of the investigated steels both before and after heat treatments. The results demonstrate that in

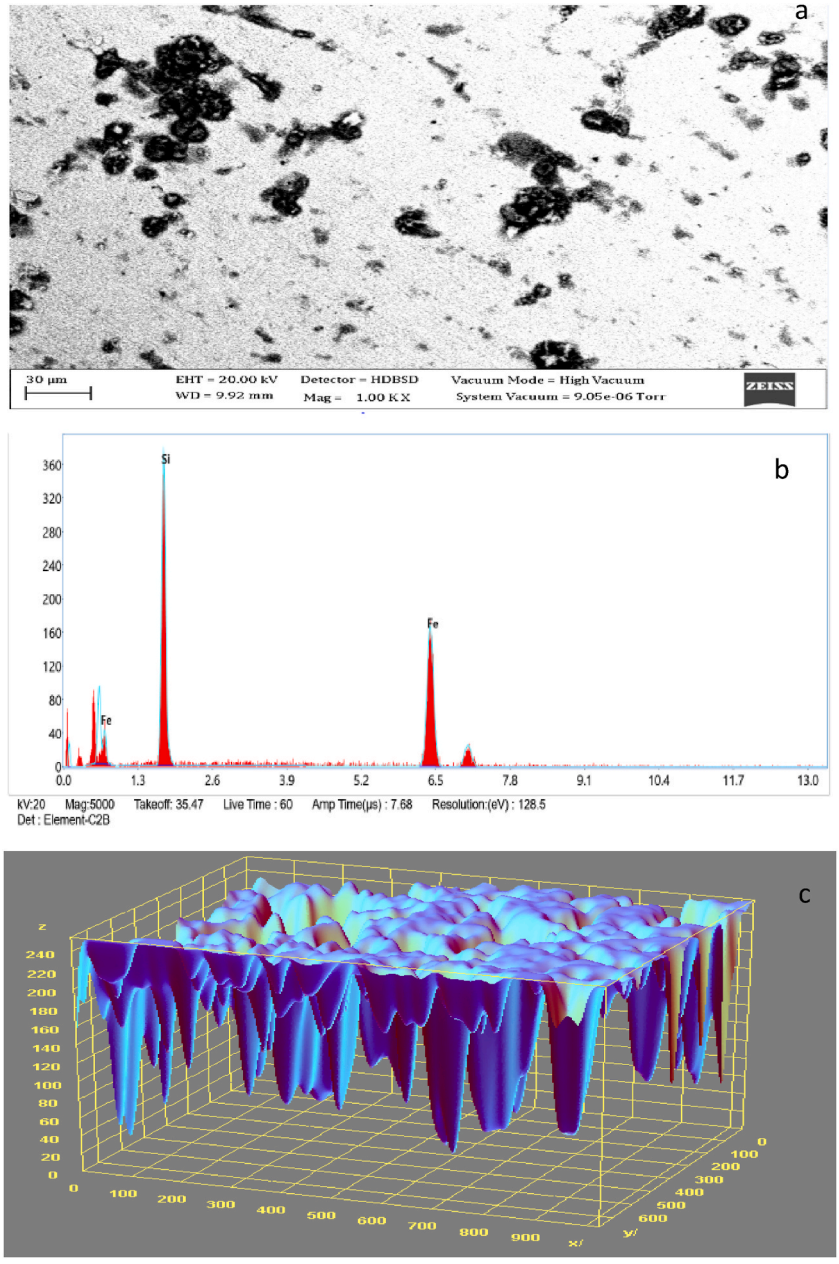

Fig. 13. a. Micrograph of medium carbon steel carburised with palm kernel shell at 1000 °*C* for 3 h. b. Energy Dispersive Spectroscopy of the elements c. 3D image of the scanning electron microstructural feature of the steel sample.

its as-received state, carburised steel is harder than uncarburised steel. This hardness has also been improved by heat treatments. Carburised steel's hardness was increased from 80.4 H V in the as-received state to 161.5 H V following heat treatment at 1050 °C/3 h with finely ground palm kernel shell. 97.5 H V following heat treatment at 1050 °C/2 h:30 min with sawdust, 131.5 H V following heat treatment at 1050 °C/2 h:30 min with coconut shell and sawdust, 135 H V following heat treatment at 1100 °C/2 h:30 min with coconut shell and sawdust,119.5 H V following heat treatment at 1100 °C/3 h with sawdust, 161.5 H V following heat treatment at 1050 °C/3 h with palm kernel shell, 84.5 H V following heat treatment at 900 °C/1 h sawdust, 127 H V following heat treatment at 900 °C/1 h with palm kernel shell, and sawdust, 137 H V following heat treatment at 900 °C/2 h with palm kernel shell, and sawdust, 145.5 H V following heat treatment at 950 °C/2 h with palm kernel shell, coconut shell and sawdust and 151.5 H V following heat treatment at 900 °C/1 h with palm kernel shell, sawdust, and coconut shell respectively. The effect of the additional carbon elements accounts for the increase in hardness of the hammer material compared to the steel in the as-received state. Niobium and chromium are referred to as carbide-forming elements. The hardness is increased by their dispersion in the microstructure. Martensite development in the heat-treated state justifies an increase in hardness. Due to the transformation of austenite to martensite during high-temperature

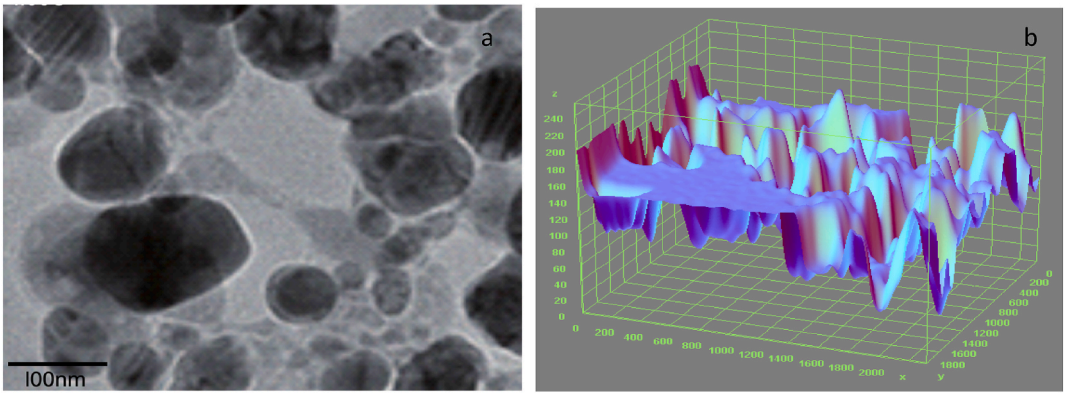

Fig. 14. a. TEM Micrograph of the steel sample carburised with palm kernel shell at 1050 °*C* for 3 h b 3D surface plot image of the transmission electron microstructural feature of the steel sample carburised.

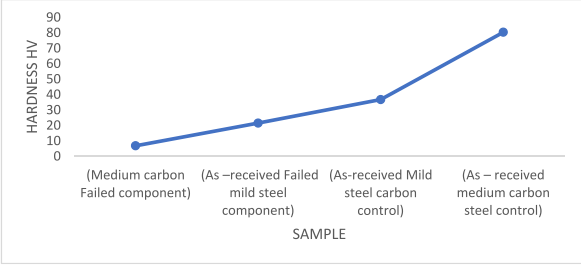

Fig. 15. Hardness values of as-received samples.

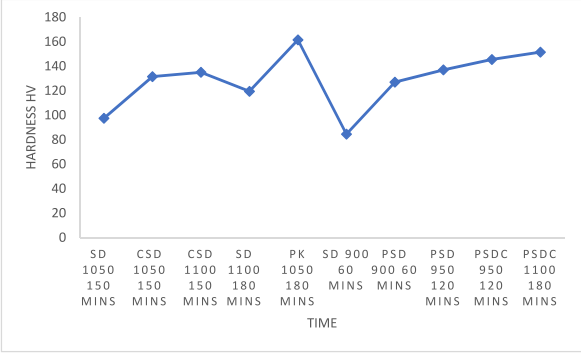

Fig. 16. Hardness values of carburised samples at different temperatures and time using coconut shell, sawdust, and palm kernel shell at different variations.

austenization and water quenching, the steel undergoes a microstructural change that increases its hardness. The steel is further strengthened by the inclusion of substances that make steel more hardenable, such as chromium and niobium [20,21]. Furthermore, optimal results are achieved at 1050 °C for 180 mins as compared with 900 °C, 950 °C,1000 °C carburising temperatures. According to the microstructural investigation, heating to 1050 °C with finely crushed palm kernel shell caused more secondary carbides created during solidification to dissolve. A richer and tougher martensite is created as a result of the carbon diffusion into the sample.

3.15. Wear analysis

The wear volume and rate for each sample were measured at a particular varied time (90–150) mins during carburisation and the results were displayed in Table 4.

The specimen's volume loss (V) is calculated as follows:

Table 4
Results of metal sample weight loss and wear volume.

METAL SAMPLE	TEMP (°C)	TIME (min)	METAL SAMPLE WEIGHT LOSS (x 10^{-3} kg)	METAL SAMPLE WEAR VOLUME (× $10^{-3}m^3$)
1	900	90	0.001	0.001
2	950	90	0.05	0.00246
3	1000	90	0.088	0.00974
4	1050	90	0.017	0.00161
5	900	120	0.004	0.00022
6	950	120	0.0122	0.00228
7	1000	120	0.042	0.0038
8	1050	120	0.028	0.0028
9	900	150	0.043	0.005
10	950	150	0.091	0.011
11	1000	150	0.052	0.006
12	1050	150	0.08	0.00508

$$\Delta V = \frac{(W1 - W2)}{\rho} \times 1000 \tag{1}$$

where, ρ = Experimental density of the sample.

The Specific wear rate (W_s) of the sample is calculated as follows:

$$W_s = \frac{\Delta V}{F_N \times S_S} \tag{2}$$

where S_S = Sliding distance (mm),
F_N = Normal load (N) = 10 N

$$\text{Wear resistance} = \frac{\text{Sliding Distance (S)}}{Volume\ (Vloss \times 1000)} \tag{3}$$

When carburising temperatures rise and the carbon in the carburiser has not yet reached saturation to dissipate into the core layer of the crushing materials, the amount of weight loss increases in polynomials trend form, as shown in Figs. 17–19. However, this changes as the temperature approaches the holding temperature of 900 °C. Aside from the fact that the lowest weight loss was obtained in Fig. 17 for sample 5 of holding temperature and time 1000 °C and 90 min, it is evident from Fig. 20 that a high wide range of low in weight loss was encountered.

In Figs. 20–22, the wear rate and carburising temperature's polynomial trending behavior acquired a new dimension. The best wide range of low wear rates were discovered in Figs. 21 and 22, which may be due to the high saturation temperature and time that gave the carburiser adequate strength to diffuse more quickly into the surfaces of the materials used in metal sample (crushing tools).

3.16. Thermal gravimetric analysis

Thermal gravimetric analysis is a crucial technique utilized in this study to describe and evaluate the thermal stability of the hammer materials. The weight variation of the sample was tracked and calculated as a function of temperature and time. But when put under a controlled temperature program of 30.00 °C–950.00 °C at 10.00 °C/min in a service environment, useful information on the

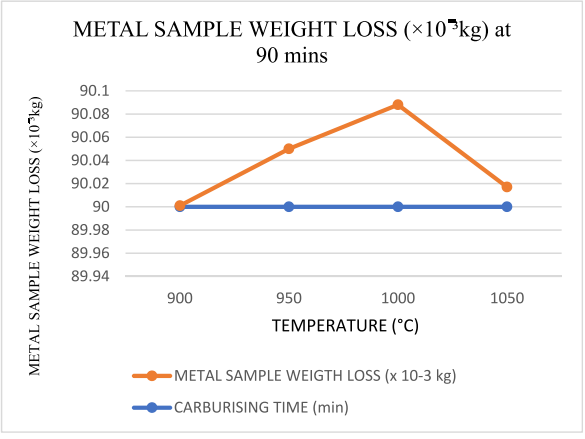

Fig. 17. Carburising temperature dependence of metal sample (crushing tool) weight loss at 90 min s

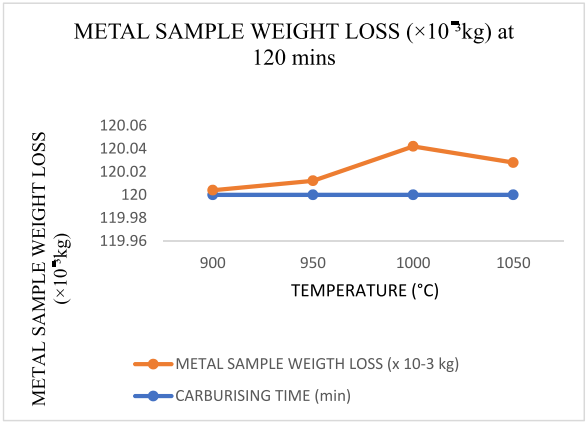

Fig. 18. Carburising temperature dependence of metal sample (crushing tool) weight loss at 120 min s

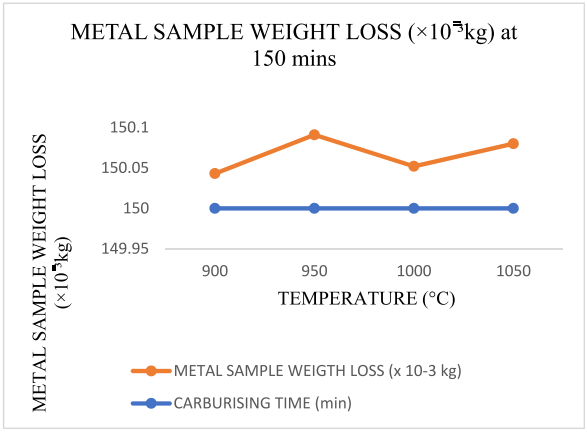

Fig. 19. Carburising temperature dependence of metal sample (crushing tool) weight loss at 150 min s

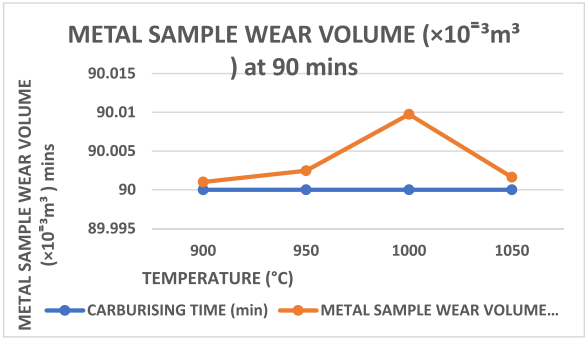

Fig. 20. Carburising temperature dependence on wear volume at 90 min s

thermal decomposition was recorded. Fig. 23, depicts the DTG curves of a sample that was carburised for 180 min at 1050 °C, and demonstrates the sample's much higher thermal stability. The outcome showed that the rate of mass loss for the sample decreased with temperature and rose much less.

4. Conclusion

According to the material's elemental composition, case hardening and stress relief techniques were employed for the funtionalisation of the crushing material. The evaluation of bone-crushing machine performance in terms of strength properties and tribological

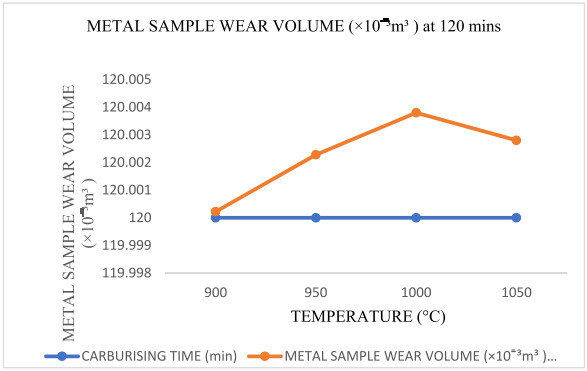

Fig. 21. Carburising temperature dependence on wear volume at 120 min s

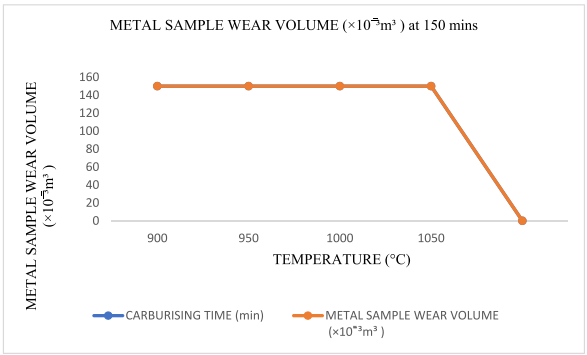

Fig. 22. Carburising temperature dependence on wear volume at 150 min s

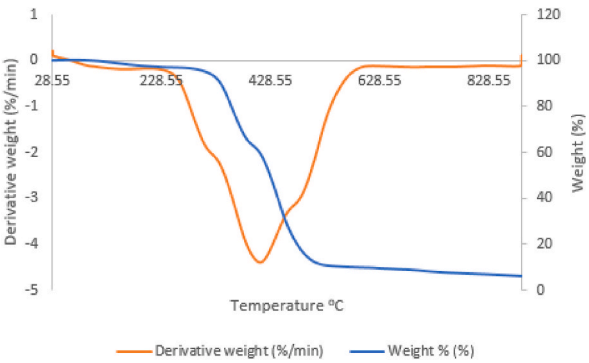

Fig. 23. TGA/DTA Curve of samples caaburised with palm kernel shell at 1050 °*C* and 180 min.

behavior was investigated. The results showed that the finely ground agro waste improved the hammer material's performance with greater efficiency. Additionally, hardness and microstructural property investigations were performed to ascertain the extent to which the agro waste affected the composition of alloying element present in the sample. The results of the thermal gravimetric analysis tests demonstrated the beneficial effect of the finely ground palm kernel shell on the thermal performance of the crushing material, while the results of the wear tests demonstrated the influence of agro waste on the capacity to resist wear. However, the significance of agro waste in the heat treatment process cannot be overlooked in engineering application systems. It has now enthralled its position in the area of viable industrial applications. The functionalization of medium carbon steel for improved mechanical properties could essentially broaden its applications.

5. Current research limitations and future directions

The research and findings also suggest that there are a number of possible future directions for resolving other industrial challenges

of a like nature. Future research on this topic will concentrate on the following limitations.

- The effects of the elements' alloying percentages after the elements' compounds are formed or after the elements are incorporated into the steel
- local design and production of a crushing machine with improved service life using eco-friendly and economically efficient agro waste for industrial application
- Conduct performance evaluation tests to support the viability of the proposed solution

Declaration of competing interest

The authors declare that they have no known competing financial interests or personal relationships that could have appeared to influence the work reported in this paper

Acknowledgments

We hereby acknowledge the financial support of Covenant University, Ota, Ogun State. Nigeria for publication.

References

[1] S. Rashid, O. Bashir, I. Majid, Different mechanical conveyors in food processing, in: Transporting Operations of Food Materials within Food Factories, Woodhead Publishing, 2023, pp. 253–263.
[2] U. Wendt, Engineering materials and their properties, in: Springer Handbook of Mechanical Engineering, Springer, Cham, 2021, pp. 233–292.
[3] Q. Chao, S. Thomas, N. Birbilis, P. Cizek, P.D. Hodgson, D. Fabijanic, The effect of post-processing heat treatment on the microstructure, residual stress and mechanical properties of selective laser melted 316L stainless steel, Mater. Sci. Eng. 821 (2021), 141611.
[4] I. Burda, K. Zweiacker, A. Arabi-Hashemi, P. Barriobero-Vila, A. Stutz, R. Koller, C. Leinenbach, Fatigue crack propagation behavior of a micro-bainitic TRIP steel, Mater. Sci. Eng. 840 (2022), 142898.
[5] H. Yu, Z. Wang, J. Yuan, Loosening and fracture behavior of hybrid titanium-to-steel threaded connection under cyclic loading condition, Eng. Fail. Anal. 142 (2022), 106742.
[6] S. Manghnani, D. Shekhawat, C. Goswami, T.K. Patnaik, T. Singh, Mechanical aan tribological characteristics of Si3N4 reinforced aluminium matrix composites: a short review, Mater. Today: Proc. 44 (2021) 4059–4064.
[7] M. Ramesh, L. Rajeshkumar, D. Balaji, V. Bhuvaneswari, Green composite using agricultural waste reinforcement, in: Green Composites, Springer, Singapore, 2021, pp. 21–34.
[8] J. Du, J. Li, Y. Feng, J. Ning, S. Liu, F. Zhang, Effect of layered heterogeneous microstructure design on the mechanical behavior of medium carbon steel, Mater. Des. 221 (2022), 110953.
[9] B. Avishan, P. Talebi, S. Tekeli, S. Yazdani, Producing nanobainite on surface of a low-carbon low-alloy steel, J. Mater. Eng. Perform. (2022) 1–10.
[10] J.L. Ling, W.Y. Liew, N.J. Siambun, J. Dayou, Y.Y. Lim, Z.T. Jiang, Sliding wear of electro- mild steel with different microstructures, Tribol. Mater. Surface Interfac. 15 (3) (2021) 213–228.
[11] J. Weise, D. Lehmhus, J. Sandfuchs, M. Steinbacher, R. Fechte-Heinen, M. Busse, Syntactic iron foams' properties tailored by means of case hardening via carburizing or carbonitriding, Materials 14 (16) (2021) 4358.
[12] A. Chamanfar, S.M. Chentouf, M. Jahazi, Boire Lapierre, L. P, Austenite grain growth and hot deformation behavior in a medium carbon low alloy steel, J. Mater. Res. Technol. 9 (6) (2020) 12102–12114.
[13] U. Gürol, S.C. Kurnaz, Effect of carbon and manganese content on the microstructure and mechanical properties of high manganese austenitic steel, J. Min. Metall. B Metall. 56 (2) (2020) 171–182.
[14] S.F. Lütke, A.V. Igansi, L. Pegoraro, G.L. Dotto, L.A. Pinto, T.R. Cadaval Jr., Preparation of activated carbon from black wattle bark waste and its application for phenol adsorption, J. Environ. Chem. Eng. 7 (5) (2019), 103396.
[15] E.E.T. Elsawy, M.R. El-Hebeary, I.S.E. El Mahallawi, Effect of manganese, silicon and chromium additions on microstructure and wear characteristics of grey cast iron for sugar industries applications, Wear 390 (2017) 113–124.
[16] H. Xue, W. Peng, L. Yu, R. Ge, D. Liu, W. Zhang, Y. Wang, Effect of hardenability on microstructure and property of low alloy abrasion-resistant steel, Mater. Sci. Eng. 793 (2020), 139901.
[17] S.T. Zhou, Z.D. Li, L. Jiang, X. Wang, P. Xu, Y.X. Ma, Q.L. Yong, An investigation into the role of non-metallic inclusions in cleavage fracture of medium carbon pearlitic steels for high-speed railway wheel, Eng. Fail. Anal. 131 (2022), 105860.
[18] P.M. Kaikkonen, M.C. Somani, L.P. Karjalainen, J.I. Kömi, Flow stress behaviour and static recrystallization characteristics of hot deformed austenite in microalloyed medium-carbon bainitic steels, Metals 11 (1) (2021) 138.
[19] Wu Ramli, C. C, A. Shaaban, Mechanical properties of pack carburized SCM 420 steel processed using natural shell powders and extended carburization time, Crystals 11 (9) (2021) 1136.
[20] O.O. Joseph, K.O. Babaremu, Agricultural waste as a reinforcement particulate for aluminum metal matrix composite (AMMCs): a review, Fibers 7 (4) (2019) 33.
[21] E.Y. Salawu, A.A. Adediran, O.O. Ajayi, A.O. Inegbenebor, J.O. Dirisu, On the analyses of carbon atom diffused into grey cast iron during carburisation process, Sci. Rep. 12 (1) (2022) 18303.